



Contents lists available at ScienceDirect

Bioorganic & Medicinal Chemistry Letters

journal homepage: www.elsevier.com/locate/bmcl

Discovery of dihydroisoquinolinone derivatives as novel inhibitors of the p53–MDM2 interaction with a distinct binding mode

François Gessier, Joerg Kallen, Edgar Jacoby, Patrick Chène, Thérèse Stachyra-Valat, Stephan Ruetz, Sébastien Jeay, Philipp Holzer, Keiichi Masuya, Pascal Furet*

Novartis Institutes for BioMedical Research, WKL-136.P.12, CH-4002 Basel, Switzerland

ARTICLE INFO

Article history:

Received 28 May 2015

Accepted 16 June 2015

Available online xxxx

Keywords:

MDM2

p53

Protein–protein interaction inhibitors

ABSTRACT

Blocking the interaction between the p53 tumor suppressor and its regulatory protein MDM2 is a promising therapeutic concept under current investigation in oncology drug research. We report here the discovery of the first representatives of a new class of small molecule inhibitors of this protein–protein interaction: the dihydroisoquinolinones. Starting from an initial hit identified by virtual screening, a derivatization program has resulted in compound **11**, a low nanomolar inhibitor of the p53–MDM2 interaction showing significant cellular activity. Initially based on a binding mode hypothesis, this effort was then guided by a X-ray co-crystal structure of MDM2 in complex with one of the synthesized analogs. The X-ray structure revealed an unprecedented binding mode for p53–MDM2 inhibitors.

© 2015 Elsevier Ltd. All rights reserved.

Reactivating the p53 tumor suppressor is an attractive therapeutic concept in oncology.¹ In particular, in cancer cells overexpressing MDM2, the main negative regulator of p53, blocking the interaction between the two proteins is a strategy under intense investigation to reactivate the tumor suppressor.² This line of research has led to several small molecule p53–MDM2 interaction inhibitors in clinical evaluation.³ Our group has been involved in this effort since the early peptide work and so far we have disclosed two new classes of potent non peptide p53–MDM2 interaction blockers resulting from our medicinal chemistry program in this area of anticancer drug research.^{4–6} In this Letter, we report the discovery of a third new class of p53–MDM2 inhibitors: the dihydroisoquinolinones.

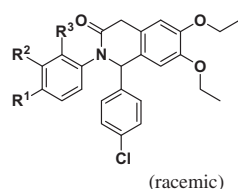
The starting points of our previously reported p53–MDM2 inhibitors were identified by structure-based design. More precisely, they were designed according to the ‘central valine’ concept.⁵ The latter consists in placing a planar aromatic or hetero-aromatic core moiety within van der Waals distance of V93, a residue occupying a central position in the p53 binding pocket of MDM2.⁷ This provides appropriate exit vectors on the core scaffold to attach substituents that efficiently occupy the three essential sub-pockets of the MDM2 cleft involved in the recognition of residues Phe 19, Trp 23 and Leu 26 of the transactivation domain of p53.⁸

In addition to structure-based design, we have resorted to virtual screening in our search for new p53–MDM2 inhibitor

chemotypes. Following a procedure previously published which involved a combination of several 2D and 3D virtual screening methods, around 50,000 compounds from the Novartis compound collection were selected for testing in our p53–MDM2 program.⁹ From this effort, compound **1** (Table 1) was identified as an interesting hit inhibiting the p53–MDM2 interaction with an IC₅₀ value of 0.54 μM in our TR-FRET biochemical assay and showing a weak anti proliferative activity of 16.5 μM at the cellular level.^{10,11} Compound **1** was considered to be an attractive starting point for further exploration. To guide the design of analogs, we sought the most plausible hypothesis for the binding mode of compound **1** in the p53 binding pocket of MDM2. Docking studies, combined with the pharmacophore knowledge obtained from our previous classes of p53–MDM2 inhibitors, led to the binding model shown in Figure 1.¹² In this model, conforming to our ‘central valine’ concept, the dihydroisoquinolinone core of the compound in a semi-boat conformation makes extensive van der Waals contacts with the side chain of MDM2 residue V93. Such a position of the bicyclic core in the cavity allows the ethoxy substituents and the chlorophenyl ring, in a pseudo-equatorial orientation, to occupy the Trp 23 and Phe 19 sub-pockets, respectively, while the methoxyphenyl ring forms an aromatic π–π stacking interaction with residue H96 in the Leu 26 sub-pocket.¹³ In addition, the compound carbonyl group accepts a hydrogen bond from the imidazole ring of H96. These interactions with H96 had been observed in crystal structures of MDM2 in complex with our previous p53–MDM2 inhibitors.⁶ Moreover, a chlorophenyl moiety filling the Trp 23 sub-pocket is a hallmark of p53–MDM2 inhibitors. This binding

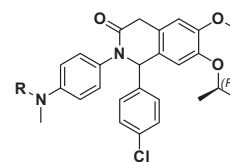
* Corresponding author. Tel.: +41 61 696 79 90; fax: +41 61 696 48 70.

E-mail address: pascal.furet@novartis.com (P. Furet).

Table 1
Biochemical activity of compounds 1–3 and 5

Compound	R ¹	R ²	R ³	TR-FRET IC ₅₀ (μM)
1	Methoxy	H	H	0.54 ± 0.08
2	Cl	H	H	1.0 ± 0.1
3	H	Cl	H	1.4 ± 0.3
5	Methyl	H		0.38 ± 0.05

The IC₅₀ values are averages of at least 2 separate determinations.

Table 2
Biochemical activity of compounds 4 and 6–9

Compound	R	TR-FRET IC ₅₀ (μM)
4	Methyl	0.12 ± 0.02
6		0.17 ± 0.05
7		0.12 ± 0.01
8		0.015 ± 0.003
9		0.008 (n = 1)

The IC₅₀ values are averages of at least 2 separate determinations.

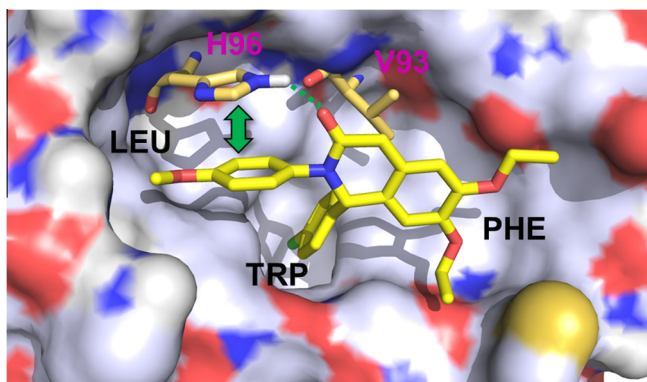


Figure 1. Initial binding model of compound 1 in the MDM2 cavity. The three MDM2 sub-pockets are labeled PHE (Phe 19), TRP (Trp 23) and LEU (Leu 26). The putative interactions with H96, hydrogen bond and π - π stacking, are represented by a dashed line and an arrow, respectively.

model was thus consistent with the available crystallographic and pharmacophore information.

We started the optimization of compound 1 by the synthesis of analogs 2 and 3 in which the *para*-methoxy group of the parent compound was replaced by a *para*-chloro and *meta*-chloro substituent, respectively. Based on the binding model and the structure–activity relationships of our previous classes of p53–MDM2 inhibitors, chloro substituents on the phenyl ring occupying the Leu 26 sub-pocket were expected to improve potency. However, compounds 2 and 3 turned out to be around two-fold less active than 1 in the biochemical assay (Table 1). These results prompted us to envisage a more systematic investigation of the dihydroisoquinolinone scaffold to further probe the binding mode hypothesis. A number of derivatives with diverse variations at the ether positions and various substitutions with small groups on the phenyl ring assumed to bind in the Leu 26 sub-pocket were prepared. We obtained structure–activity relationships indicating that the ether positions were rather tolerant to the diverse substitutions tried with a slight preference for small aliphatic groups. As for substitutions on the phenyl ring, there was a clear preference for a *para* substituent over an *ortho* or *meta* one. At the end of this investigation, the most potent compound obtained was 4, having an IC₅₀ value of 0.12 μM in the biochemical assay (Table 2). Although the binding model could largely account for the structure–activity relationships observed at the ether

positions, it could not satisfactorily explain the preference for *para* substituents on the Leu 26 sub-pocket phenyl ring, in particular for the dimethyl amino substituent present in compound 4. At this point, we decided to focus our efforts on obtaining a crystal structure of MDM2 in complex with a representative of our dihydroisoquinolinone inhibitors to elucidate their binding mode. Our initial attempts at co-crystallizing MDM2 with inhibitors were hampered by their low solubility, a high compound concentration being required in such experiments. To identify suitable tool compounds for the co-crystallization trials, solubilizing tags were introduced at several positions of the inhibitor chemotype. Most of these modifications, although improving solubility, led to some loss of potency reducing the chances of obtaining a co-crystal. However, with compound 5 (Table 1) an adequate balance of solubility/potency was reached for successful co-crystallization. It resulted in the first crystal structure of MDM2 in complex with one of the dihydroisoquinolinone inhibitors.

The X-ray co-crystal structure of the MDM2/compound 5 complex is shown in Figure 2.¹⁴ To our surprise, it revealed an unprecedented type of binding mode in which the inhibitor bicyclic core makes hydrophobic contacts with residues I54, F55 and G58 of helix α 2 of MDM2 rather than interacts with V93 as proposed in the binding model. This novel type of binding mode appears facilitated by a different side chain conformation of F55 compared to that observed for this residue in all previously reported MDM2 crystal structures available in the PDB database. In the latter, the χ_1 torsion angle of F55 corresponds to a *t* rotamer which allows the formation of an intramolecular face to edge aromatic interaction with Y56, a neighboring residue. In contrast, in the complex with compound 5, a *g*⁻ rotameric state for χ_1 brings the side chain of F55 into closer proximity to the center of the MDM2 cavity where it can contact the inhibitor. Besides the core interactions, the three MDM2 sub-pockets determining binding affinity are occupied by the inhibitor. The deepest one, Trp 23, is filled by the compound chlorophenyl ring projecting with a pseudo-axial orientation from the dihydroisoquinolinone core in a semi-boat conformation. Hence, compound 5 conforms to the usual Trp 23 sub-pocket pharmacophore. However, it is not the case for the other sub-pockets. Unlike our previous series of inhibitors, 5 does not form an aromatic π - π stacking interaction with residue H96 of the Leu 26 sub-pocket. The compound occupies this sub-pocket

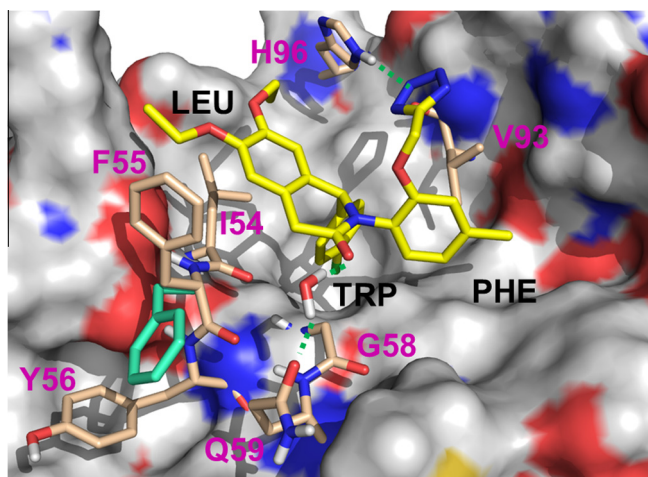


Figure 2. Crystal structure of MDM2 in complex with compound **5** (PDB code: 4ZYC). The hydrogen bond between the inhibitor tetrazole ring and H96 appears as a dashed line. A water mediated hydrogen bond existing between the carbonyl group of the inhibitor bicyclic core and residue Q79 is represented in the same manner. The conformation of the side chain of F55 usually observed in crystal structures of MDM2 is shown in green. The crystal structure indicates that the MDM2 pocket is occupied by the enantiomer of **5** with the (*S*) configuration at the chiral center.

with one of its two ethoxy substituents, the other one making hydrophobic contacts with the side chain of F55 in addition to those made by the bicyclic core with this residue. Still, an interaction with H96 is observed but it does not involve the moiety engaging the Leu 26 sub-pocket. In fact, H96 donates a hydrogen bond to the tetrazole ring of the solubilizing tag attached to the inhibitor tolyl group which inserts in the Phe 19 sub-pocket. Overall, a new way of interacting with the p53 binding cleft of MDM2 was revealed by this crystal structure. It gave a new basis to the optimization of our dihydroisoquinolinone inhibitors.

Using a model of compound **4** docked in the MDM2 cavity with the same binding mode as that of compound **5** in the crystal structure (Fig. 3), new analogs of the former compound were designed.¹⁵ Examination of the model suggested opportunities to enhance binding interactions with MDM2 in the Phe 19 sub-pocket by replacing one of the methyl groups of the dimethylamino substituent of **4** by a larger group. In particular, this position of the compound offered an appropriate vector to target Y67, a well exposed residue of the Phe 19 sub-pocket. On this basis, compounds **6–9** (Table 2) were designed to form aromatic interactions

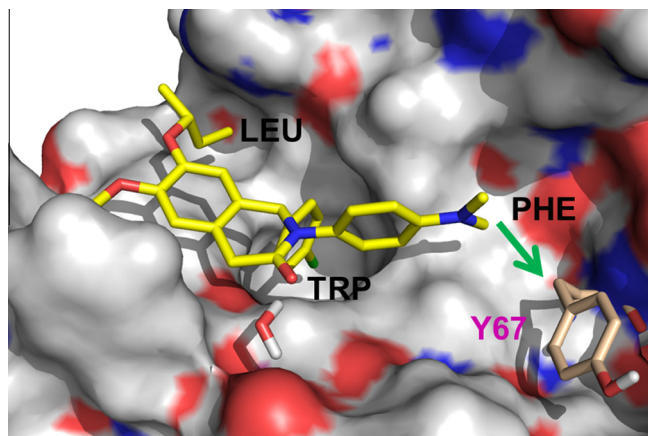


Figure 3. Compound **4** docked in the MDM2 pocket. The green arrow indicates the direction of derivatization to interact with residue Y67 of the Phe 39 sub-pocket.

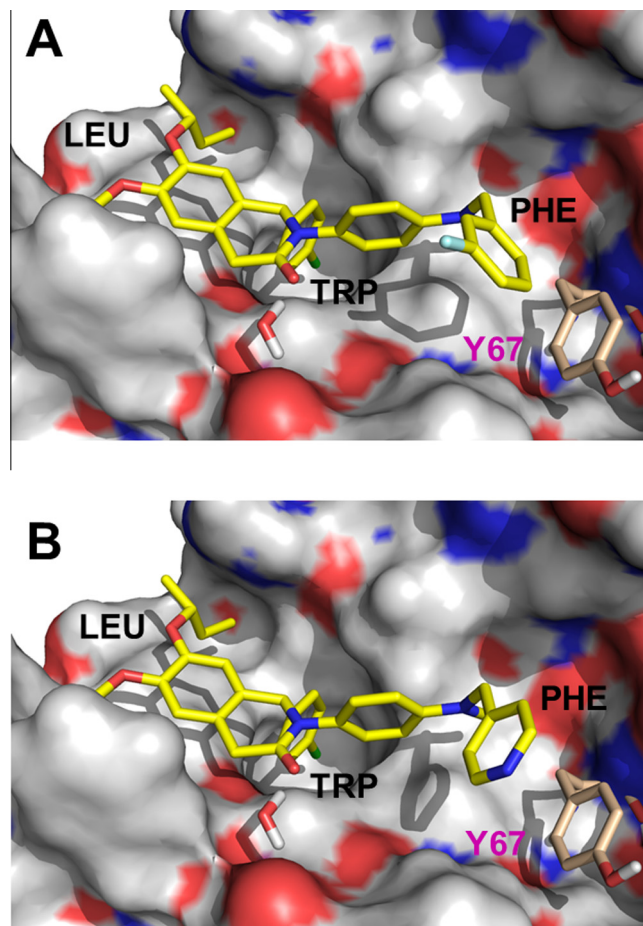
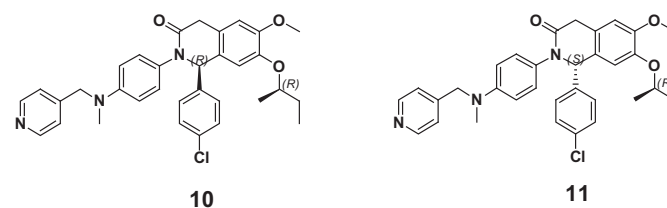


Figure 4. (A) Model of MDM2 in complex with **6** in which the compound fluorophenyl ring makes an aromatic face to edge interaction with the phenol ring of Y67. (B) Model of MDM2 in complex with **9** in which the compound pyridyl ring makes a π - π stacking interaction with the phenol ring of Y67.

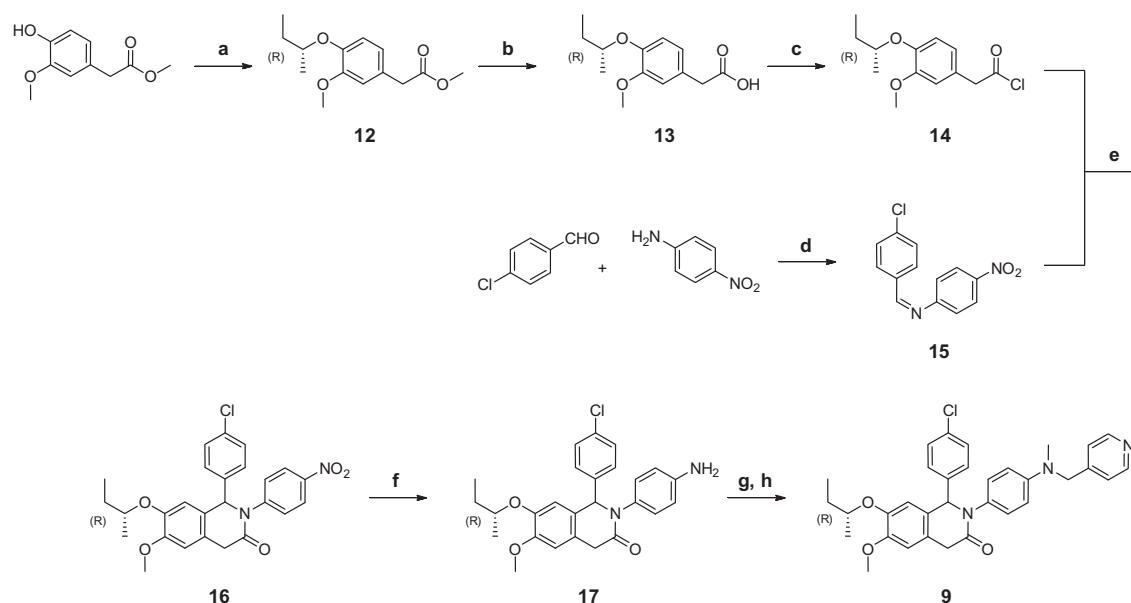
Table 3
Biochemical and cellular activity of compounds **10** and **11**



Compound	TR-FRET IC ₅₀ (μM)	SJSA-1 IC ₅₀ (μM)	SAOS-2 IC ₅₀ (μM)
10	1.2 ± 0.3	29.6 (n = 1)	>30
11	0.0023 ± 0.0004	1.2 ± 0.3	12 ± 5

The IC₅₀ values are averages of at least 2 separate determinations.

with the phenol ring of Y67. Modeling indicated that a group of the benzylic type attached to the *para* amino substituent of **4** could interact with the phenol ring of Y67 either in a π - π stacking orientation or a face to edge one. Both types of aryl-aryl interaction are strengthened by introducing electron withdrawing substituents or heteroatoms in the ring having as partner an electron rich aromatic system such as phenol.¹⁶ This is why fluorophenyl and pyridine rings were chosen in compounds **6–9** to interact with Y67. An illustration of these design ideas is given in Figure 4.



Scheme 1. Reactions and conditions: (a) (*S*)-butan-2-ol, PPh₃, DTAD, DCM, rt, quant.; (b) LiOH, EtOH, water, rt, 2 h, 71%; (c) (COCl)₂, DMF, DCM, rt, 1 h, quant.; (d) neat, rt, 3 days, 80%; (e) **14**, DCM, rt, 1 h then MeSO₃H, 0 °C, 15 min, 47%; (f) Fe, AcOH, AcOEt, water, 80 °C, 1 h, 99%; (g) isonicotinaldehyde, NaBH(OAc)₃, AcOH, DCM, rt, 3 h, 82%; (h) 37% HCHO in water, NaBH(OAc)₃, AcOH, DCM, rt, 3 h, 54%.

Compounds **6–9** were synthesized and tested in the biochemical assay (Table 2). The fluorophenyl derivatives **6** and **7** remained at the same level of potency as the parent compound **4**. However, gratifyingly, a marked improvement of activity by one order of magnitude was obtained with the pyridyl analogs **8** and **9**.¹⁷ In fact, compound **9** represented the first member of the new series reaching single digit nanomolar potency in the biochemical assay. Encouraged by this result, we decided to separate the two diastereoisomers of **9**. We obtained compounds **10** and **11** shown in Table 3 together with their activity. Based on the crystal structure of the analog **5** in complex with MDM2, we attributed the *S* configuration to the bicycle chiral center of the most active diastereoisomer **11**. This compound reached low nanomolar biochemical potency, accompanied by significant and specific inhibition of the proliferation of the p53-dependent SJS-1 cells in the low micromolar range.¹⁸ With **11**, we had reached an interesting level of cellular potency comparable to that of the reference p53–MDM2 inhibitor Nutlin-3a (IC₅₀ = 1.9 μM in the SJS-1 assay).

A representative synthesis for compound **9** is described in Scheme 1. The commercially available methyl 2-(4-hydroxy-3-methoxyphenyl)acetate was subjected to a Mitsunobu reaction with (*S*)-butan-2-ol using DTAD and triphenylphosphine as reagents to deliver the *sec*-butyl ether **12** as its pure (*R*)-enantiomer. The methyl ester functionality of **12** was hydrolyzed with LiOH into the corresponding carboxylic acid **13** which reacted with oxalyl chloride to give the acyl chloride **14** in quantitative yields. The cyclo-addition of **14** with the imine **15**, obtained from the condensation of the commercially available 4-chlorobenzaldehyde and 4-nitroaniline, led to the dihydroisoquinolinone analog **16** with no stereo-selectivity observed for the newly created asymmetric center. The nitro group of **16** was reduced with iron following classical reaction conditions to give the corresponding aniline **17** in nearly quantitative yields. Finally, the aniline functionality underwent two consecutive reductive aminations with isonicotinaldehyde and formaldehyde, respectively, using NaBH(OAc)₃ as a reducing agent to deliver compound **9** as a mixture of two diastereoisomers. At that point, the separation of the diastereoisomer pair could not be achieved by classical normal phase or reversed phase

chromatography and required the use of chiral chromatography conditions.

In conclusion, improvements to a virtual screening hit have led to the first potent representatives of a new class of inhibitors of the p53–MDM2 interaction based on a dihydroisoquinolinone scaffold. A crystal structure shows that the new inhibitors adopt a different binding mode in the MDM2 cavity compared to all the inhibitors reported in the literature. The potent inhibitor **11** has been the starting point of another round of medicinal chemistry optimization that has culminated in NVP-CGM097, a compound currently under evaluation in a phase I clinical trial for cancer patients.^{19,20}

References and notes

- Selivanova, G. *FEBS Lett.* **2014**, *588*, 2628.
- For recent reviews on the topic see: (a) Lv, P.-C.; Sun, J.; Zhu, H.-L. *Curr. Med. Chem.* **2015**, *22*, 618; (b) Nag, S.; Zhang, X.; Wang, M.-H.; Srivenugopal, K. S.; Wang, W.; Zhang, R. *Curr. Med. Chem.* **2014**, *21*, 553; (c) Wade, M.; Li, Y. C.; Wahl, G. M. *Nat. Rev. Cancer* **2013**, *13*, 83; (d) Li, Q.; Lozano, G. *Clin. Cancer Res.* **2013**, *19*, 34; (e) Carry, J. C.; García-Echeverría, C. *Bioorg. Med. Chem. Lett.* **2013**, *23*, 2480; (f) Zak, K.; Pecak, A.; Rys, B.; Wladyka, B.; Doemling, A.; Weber, L.; Holak, T. A.; Dubin, G. *Expert Opin. Ther. Pat.* **2013**, *23*, 425; (g) Wang, S.; Zhao, Y.; Bernard, D.; Aguilar, A.; Kumar, S. *Top. Med. Chem.* **2012**, *8*, 57; (h) Capdevila, J.; Cervantes, A.; Taberner, J. *Drugs Future* **2012**, *37*, 273; (i) Ray-Coquard, L.; Blay, J. Y.; Italiano, A.; LeCesne, A.; Penel, N.; Zhi, J.; Heil, F.; Rueger, R.; Graves, B.; Ding, M.; Geho, D.; Middleton, S. A.; Vassilev, L. T.; Nichols, G. L.; Bui, B. N. *Lancet Oncol.* **2012**, *13*, 1133; (j) Macchiarulo, A.; Giacchè, N.; Carotti, A.; Moretti, F.; Pellicciari, R. *Med. Chem. Commun.* **2011**, *2*, 455; (k) Cheok, C. F.; Verma, C. S.; Baselga, J.; Lane, D. P. *Nat. Rev. Clin. Oncol.* **2011**, *8*, 25; (l) Millard, M.; Pathania, D.; Grande, F.; Xu, S.; Neamati, N. *Curr. Pharm. Des.* **2011**, *17*, 536; (m) Brown, C. J.; Cheok, C. F.; Verma, C. S.; Lane, D. P. *Trends Pharmacol. Sci.* **2011**, *32*, 53; (n) Vu, B. T.; Vassilev, L. In *Current Topics in Microbiology and Immunology (Small Molecules Inhibitors of Protein–Protein Interactions)*; Vassilev, L., Fry, D., Eds.; Springer: Berlin Heidelberg, 2011; Vol. 348, pp 151–172; (o) Weber, L. *Expert Opin. Ther. Pat.* **2010**, *20*, 179.
- (a) Zhao, Y.; Aguilar, A.; Bernard, D.; Wang, S. *J. Med. Chem.* **2015**; (b) Hoe, K. K.; Verma, C. S.; Lane, D. P. *Nat. Rev. Drug Disc.* **2014**, *13*, 217; (c) Rew, Y.; Sun, D. J. *Med. Chem.* **2014**, *57*, 6332.
- García-Echeverría, C.; Chêne, P.; Blommers, M. J. J.; Furet, P. *J. Med. Chem.* **2000**, *43*, 3205.
- Furet, P.; Chêne, P.; De Pover, A.; Stachyra-Valat, T.; Hergovich Lisztwan, J.; Kallen, J.; Masuya, K. *Bioorg. Med. Chem. Lett.* **2012**, *22*, 3498.
- Vaupel, A.; Bold, G.; De Pover, A.; Stachyra-Valat, T.; Hergovich Lisztwan, J.; Kallen, J.; Masuya, K.; Furet, P. *Bioorg. Med. Chem. Lett.* **2014**, *24*, 2110.
- To avoid confusion the one letter code is used to name the amino acid residues of MDM2 while the three letter code is used for those of p53.

8. Kussie, P. H.; Gorina, S.; Marechal, V.; Elenbaas, B.; Moreau, J.; Levine, A. J.; Pavletich, N. P. *Science* **1996**, *274*, 948.
9. Jacoby, E.; Boettcher, A.; Mayr, L. M.; Brown, N.; Jenkins, J. L.; Kallen, J.; Engeloch, C.; Schopfer, U.; Furet, P.; Masuya, K.; Lisztwan, J. *Methods Mol. Biol.* **2009**, *575*, 173.
10. For a detailed description of the TR-FRET (Time Resolved Fluorescence Resonance Energy Transfer) biochemical assay used see: Berghausen, J.; Buschmann, N.; Furet, P.; Gessier, F.; Hergovich Lisztwan, J.; Holzer, P.; Jacoby, E.; Kallen, J.; Masuya, K.; Pissot Soldermann, C.; Ren, H.; Stutz, S. PCT Int. Appl. WO 2011076786, **2011**; Chem. Abstr. **2011**, *155*, 152537. In this assay the donor fluorophore is MDM2 (amino acid residues 2-188) tagged with a C-terminal biotin moiety in combination with a Europium labeled streptavidin. The acceptor fluorophore is a p53 derived peptide (amino acid sequence 18–26 of p53: TFSDLWKLL) labeled with the fluorescent dye Cy5. The IC₅₀ values given are means of at least two measurements. For reference, the p53–MDM2 inhibitor Nutlin-3A has an IC₅₀ of 0.01 μM in this assay.
11. Our cellular assay measures the ability of compounds to inhibit the proliferation of SJS-1 cells. These are p53 positive cancer cells in which the MDM2 gene is amplified. For control, inhibition of the proliferation of the p53-null SAOS-2 cells is also measured. A detailed description of the cellular SJS-1 and SAOS-2 proliferation assays is given in: Furet, P.; Guagnano, V.; Holzer, P.; Kallen, J.; Liao, L.; Mah, R.; Mao, L.; Masuya, K.; Schlapbach, A.; Stutz, S.; Vaupel, A. PCT Int. Appl. WO 201311105. Compound **1** inhibits the proliferation of SJS-1 and SAOS-2 cells with IC₅₀ values of 16.6 μM and 19.6 μM, respectively. Compounds with micromolar/submicromolar biochemical activity such as **1** do not usually show a significant specific antiproliferative effect on SJS-1 cells. Nanomolar biochemical activity is required for this.
12. Modeling and docking was performed with a version of MacroModel enhanced for graphics by A. Dietrich. MacroModel: Mohamadi, F.; Richards, N. G. J.; Guida, W. C.; Liskamp, R.; Lipton, M.; Caufield, C.; Chang, G.; Hendrickson, T.; Still, W. C. *J. Comput. Chem.* **1990**, *11*, 440. The compounds were manually constructed and docked in the MDM2 pocket (PDB structure 4OQ3) and the resulting ligand–protein complexes energy-minimized using the AMBER*/H₂O/GBSA force field.
13. Ab initio calculations in Jaguar (Schrödinger Inc.) at the B3LYP/6-31G** level indicate that in the lowest energy conformation of **1**, the chlorophenyl ring is pseudo-axial. The pseudo-equatorial conformation is less stable by 1.6 kcal/mol. Since **1** is not a highly potent inhibitor, we judged plausible that it does not bind to MDM2 in its lowest energy conformation. A conformational energy penalty to binding of a bit more than 1 kcal/mol can be compensated by a few favorable van der Waals contacts with the binding site.
14. Kallen, J. et al. The details of this X-ray structure determination (solved at 1.95 Å resolution) will be published elsewhere. The coordinates have been deposited with PDB ID code 4ZYC.
15. Compound **4** was aligned on **5** in the crystal structure shown in Figure 2 and after removal of **5** the resulting complex was energy minimized using the procedure described in note 12.
16. Salonen, L. M.; Ellermann, M.; Diederich, F. *Angew. Chem., Int. Ed.* **2011**, *50*, 4808.
17. The reason why the fluorophenyl analogs did not lead to a gain in activity is not clear. Docking based on the crystal structure suggests that the fluorophenyl rings can make good van der Waals contacts with Y67 or possibly the adjacent residue M62. In the spirit of our design hypothesis, one could conclude that introduction of heteroatoms in the ring interacting with the phenol ring of Y67 is more efficient than electron withdrawing substituents to produce a favorable aryl–aryl contact.
18. In line with our previous experience, at least two orders of magnitudes in potency are lost going from a biochemical to a cellular setting. As the consequence of the p53–MDM2 auto-regulatory loop existing in cells, the accumulation of p53 caused by the inhibitors triggers an increase of cellular MDM2 levels which reduces inhibitor potency. See for example: Lahav, G. In *Cellular Oscillatory Mechanisms*; Maroto, M., Monk, N. A. M., Eds.; Landes Bioscience and Springer Science, 2008; pp 28–38. The fact that in cells, the inhibitors compete with full length p53 instead of the truncated form used in the biochemical assay is also likely to contribute to this loss of potency.
19. Jeay, S.; Berghausen, B.; Buschmann, N.; Chène, P. Cozens, R.; Erdmann, D.; Ferretti, S.; Furet, P.; Gabriel, T.; Gessier, F.; Graus-Porta, D.; Hofmann, F.; Holzer, P.; Ito, M.; Jacoby, E.; Jensen, M.; Kallen, J.; Lang, M.; Lisztwan, J.; Murakami, M.; Pissot-Soldermann, C.; Ruetz, S.; Rynn, C.; Sterker, D.; Stutz, S.; Valat, T.; Wiesmann, M.; Masuya, K. Discovery of NVP-CGM097, A Highly Potent and Optimized Small Molecule of MDM2 Under Evaluation in a Phase I Clinical Trial. In: Proceedings of the 105th Annual Meeting of the American Association for Cancer Research; 2014 Apr 5–9; San Diego. Philadelphia (PA): AACR; *Cancer Res.* **2014**; *74*: Abstract nr 1797.
20. The optimization of compound **11** towards a clinical candidate will be reported elsewhere.